Int. J. Nanosci. Nanotechnol., Vol. 17, No. 4, Dec. 2021, pp. 209-220

Polyaniline/Fe_3O_4/Poly (Methyl Methacrylate) Nanocomposites as an Acrylic Resin Coating for Enhancement of Anticorrosion Properties of Alkyd Paints

Hamidreza Ghafouri Taleghani[1], Mohammad Soleimani-Lashkenari[2,*], Shiva Fazli[3] and Mohsen Ghorbani[4]

[1]Department of Chemical Engineering, University of Mazandarn, Babolsar, Iran
[2]Fuel Cell Electrochemistry and Advanced Material Research Laboratory, Faculty of Engineering Modern Technologies, Amol University of Special Modern Technologies, Amol, Iran
[3]Department of Chemical Engineering, Mazandaran University of Science & Technology, Babol, Iran
[4]Department of Chemical Engineering, Babol Noshirvani University of Technolgy, Babol, Iran

(*) Corresponding author: m.soleimani@ausmt.ac.ir
(Received: 09 May 2021 and Accepted: 05 September 2021)

Abstract

The exceptional application of nanocomposites containing polyaniline as a conductive polymer, poly (methyl methacrylate) (PMMA) as an acrylic resin and Fe_3O_4 nanoparticles, for corrosion protection of mild steel was reported. The synthesized nanocomposites, were characterized with different techniques. The resulting PMMA/Polyaniline/Fe_3O_4 nanocomposites were mixed with industrial alkyd paint to be employed as an anti-corrosion layer for mild steel in a NaCl solution. Accordingly, the potentiodynamic polarization and electrochemical impedance spectroscopy (EIS) were applied in order to investigate the corrosion behavior of the coated mild steel. Based on the results, the nanocomposites showed outstanding anti-corrosion properties compared with other composites coating. After investigating various compositions of the nanocomposites (3, 6, 9 and 12%) in the alkyd paint, the ideal composition related to the most favorable corrosion protection was obtained for the paint mixture comprising 6% nanocomposites.

Keywords: *Polyaniline, Fe3O4 nanoparticles, PMMA, Anti-corrosion, Electrochemical impedance.*

1. INRODUCTION

One of the most important issues that industries face is the lack of safety in equipment as well as high level of environmental pollutants released by material damages, caused by corrosion [1]. According to the study reported by National Association of Corrosion Engineers (NACE) International, "International Measures of Prevention, Application, and Economics of Corrosion Technology (IMPACT)", it was estimated that the total annual cost caused by corrosion in the world is about $2.5 trillion [2]. The most important contributing factors in material corrosion and coating damage are the nature of the aqueous environment in which materials are operating or placed [3]. When it comes to acidic media, the situation would be worse. There is no possibility to entirely prevent material from corrosion; however, new methodologies with special coating, protective metals, and corrosion inhibitors have been suggested to impede the corrosion processes, or improving the longevity of materials [4].

Among various metals, mild steel has been focused on by many researchers due to their excellent mechanical properties, that

are reasonable for many applications such as fatigue strength, fracture toughness, as well as their relatively low price [5]. Nevertheless, the poor durability of mild steel against corrosion is often problematic [6]. According to previous research works, one way to promote corrosion behavior of metals is employing coating [7]. Nowadays, the natural strength and reasonable price of polymers as an anti-corrosion coating make them valuable choices in research experiments [8]. As among, conducting polymers, such as polyaniline (PANI), are highly dispersed in a classical polymer binder and can provide numerous advantages including protecting metals against corrosion [9]. A study revealed that PANI, as a conductive polymer, and poly methyl methacrylate (PMMA) with hydrophobic properties help to prepare high active surface polymers [10]. The corrosion inhibition can be controlled through the use of PANI/PMMA polymers owing to their outstanding features such as hydrophobic nature, low poisonous behavior and facile single-step synthesis. However, polymer-based coating has poor adhesion and low thermal stability to metal surfaces, while inorganic materials, namely nanoparticles, can significantly overcome these problems [11]. Therefore, organic-mineral nanocomposite coating is associated with high mechanical and anti-corrosion properties in organic and inorganic networks [12].

In recent decades, nanotechnology and their applications were highly concentrated on by coating industries, where conventional additives and pigments are being explored to be replaced by nanoparticles in the composite coating [13]. For instance, in a research reported by Javidparvar et al. [14], Fe_3O_4 nanopigments were synthesized through a hydrothermal method. Their results showed that the surface modification of the nanoparticles had a significant effect on epoxy coating resistance against corrosion. In another study, Mammeri et al. [15] indicated that employing PMMA-SiO_2 coating, which were fabricated through a sol-gel method, resulted in desirable elastic modulus and hardness values. Moreover, an increase in SiO_2 content in the coating was responsible for more desirable elastic properties. In another research work, Ni–P and Ni–P–Al_2O_3 electroless coatings were deposited on the surface of AISI 1045 steel discs. This study suggested that the presence of Al particles in Ni–P coating network resulted in an improvement in the wear resistance and hardness of the deposits. Furthermore, the coating treated at 400 °C possessed the greatest hardness as well as wear resistance. In a research work conducted by Alirezaei et al. [16], the influence of two surfactants, namely sodium dodecyl sulphate (SDS) and dodecyl trimethyl ammonium bromide (DTAB), on the corrosion behavior of a low carbon steel substrate coated with Ni–P–TiO_2 nanoparticles was investigated. According to this study, a uniform distribution of TiO_2 nanoparticles was achieved at an optimum concentration of DTAB. Besides, an improved corrosion behavior was obtained when the nanoparticles were incorporated in the Ni–P matrix. They claimed that, as a result, Ni–P-TiO_2 coating corrosion resistant was strongly related to the type and concentration of surfactant used. According to previous works, the control of nanoparticles size and their positioning in optimal regions is the primary purpose of fabricating nanocomposites that are intrinsically prone to create substantial aggregates [17]. Hence, using surfactants and polymers, both serving as capping agents, has been recommended.

In preliminary studies a new design of different coating with various concentrations of nanopaints in a pure form or in combination with industrial paints was widely used to protect mild steel from corrosion in saline environments, and also from the diffusion of water vapor, oxygen, and ions [18].

In this study, due to the in-situ emulsion polymerization synthesis, environmental compatibility, and low-temperature coating

preparation of PMMA/PANI/Fe_3O_4 nanocomposites, these nanocomposites were investigated as a promising organic-inorganic additive. Furthermore, structural, thermal and mechanical properties of PMMA/PANI/Fe_3O_4 nanocomposite coating was evaluated. Firstly, Fourier transform infrared spectroscopy (FTIR), X-ray diffraction (XRD), scanning and transmission electron microscopy (SEM & TEM), and thermal gravimetric analysis (TGA) were employed so as to characterize the morphologies of the nanocomposite coating. Eventually, the corrosion resistance property of a different nanocomposite coating over mild steel was evaluated using electrochemical methods such as Tafel polarization and electrochemical impedance spectroscopy (EIS) in a standard saline solution.

2. MATERIALS AND METHODS

2.1. Materials

All materials using in this work were purchased from Merck, Germany. Also, aniline monomer was distilled and stored at low temperature prior to experiments. The schematic illustration of the formation and modification of PMMA/PANI/Fe3O4 nanocomposite coating is provided in Figure 1. It should be stated that, during experiments, all agents were used without further purification. Moreover, all the solutions were prepared with deionized water (DIW, 18.2 MΩ).

2.2. Synthesis of PMMA/PANI/Fe3O4 Nanocomposite Coating

2.2.1. Preparation of Fe_3O_4 Nanoparticles

Fe_3O_4 nanoparticles with a large number of exposed Fe-O groups were synthesized by a co-precipitation method. To do so, at first, a mixture containing 20 g of $FeSO_4.7H_2O$ and 40 g of $FeCl_3.6H_2O$ in 300ml distilled water under continuous stirring to form a colloidal solution. Then, 30 ml of NH_3 solution was dissolved in 170 ml deionized water and the temperature was fixed at 70°C. This solution, afterward, was drop wise added to the colloid solution, which was stirring at 70°C. The reagents had been being boiled and refluxed for 30 min, under stirring condition. Eventually, the resulting dark emulsion was separated, washed by distilled water three times, and dried at 50°C for 24 h under vacuum condition [19, 20].

2.2.2. Preparation of PANI/ Fe3O4 Nanocomposites

PANI/Fe_3O_4 nanocomposites were prepared by chemical emulsion polymerization. In this method, initially, 0.2 g of HPC was dissolved in 100 ml aqueous solution (1M H_2SO_4). Then, 1 g of KIO_3 as an oxidant and 1 g of Fe_3O_4 nanoparticles were added to stirred above aqueous solution. It took almost 30 min to completely disperse the mixture. Finally, 1 ml of freshly aniline monomer was gradually added into the resulting mixture at 800 rpm for about 6 hours. The extraction of the PANI/Fe_3O_4 nanocomposites was conducted through centrifuging at 6000 rpm for 5 min, washing with deionized water to remove the excess acid, and storing under vacuum condition at 60°C for 24 h. PANI in a conducting form, emeraldine salt (ES), was successfully obtained after observing a dark green color of all four samples [21, 22].

2.2.3. Synthesis of PMMA

PMMA as a resin was synthesized using the following procedure: 3 g of $C_{14}H_{10}O_4$ particles had been being dispersed in 20 ml MMA under sonication for 30 min until the total dissolution of $C_{14}H_{10}O_4$ particles was achieved. At the end, the solution was stirred at 400 rpm for 24 h.

2.2.4. Synthesis of PMMA/ PANI/Fe3O4

In order to synthesize PMMA/PANI/ Fe3O4 nanocomposites, a certain amount of PANI/Fe_3O_4 nanocomposites were slowly introduced into PMMA solution, and then the resulting suspension was stirred at a stirring rate of 500 rpm at room temperature

for 24 h. The resulting composites were then used as coating agent.

2.3. Substrate Processing

In this work, in order to conduct corrosion inhibition tests, the specimens were used and they were made from mild steel working electrode with the following composition (wt%): C: 0.027; Si: 0.0027; Mn: 0.34; P: 0.009; S: 0.003; Cr: 0.008; Ni: 0.03; Cu: 0.007; Al: 0.068; Nb: 0.003, Ti: 0.003, V: 0.003 and Fe balance. Mild steel specimens with a dimension of 20×20×1 mm, and 50×50×1 mm were used as substrates for the displacement of coating in electrochemical measurements. At first, all samples were treated by sanding after a disc polishing process, and subsequently were subjected to ultrasonic cleaning in an acetone solution for about 10 min. Next, they were rinsed with distilled water, following which they were washed with ethanol for a period of 10 min. They, in the next step, were activated using 50 vol.% HCl solution for 2 min, and then were dried at room temperature. Eventually, to make a comparison, the PMMA/PANI/Fe_3O_4 nanocomposite coating was used in the following two forms: (1) the pure form and (2) in combination with industrial paints at different concentrations (3, 6, 9, 12 wt. %). The nanocomposite coating was placed on the mild steel plates with a 12 mm diameter roller, and stored on a surface for 24 h to be dried at room temperature. A 3.5 wt% NaCl solution was obtained by dilution of analytical grade NaCl with double distilled water. The entire experiment was conducted in untouched solution at about 23 $^{\circ}C$.

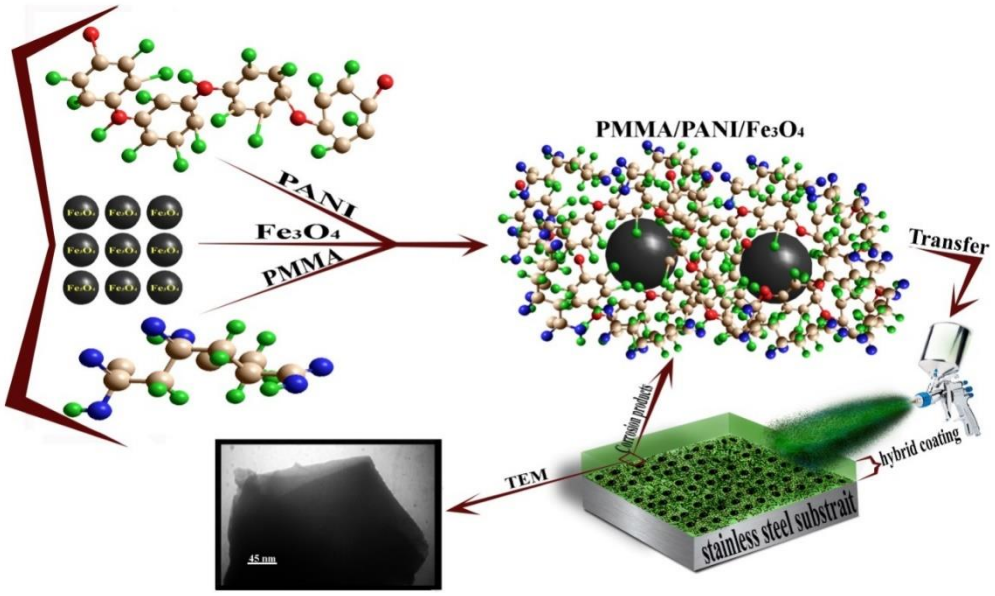

Figure 1*. The schematic diagram of PMMA/PANI/Fe3O4 nanocomposite coating preparation.*

2.4. Electrochemical Corrosion Evaluation

Corrosion experiments were performed in a three-electrode system which consisted of mild steel sheet (as working electrode), Pt wire (as auxiliary electrode), and Ag/AgCl (3 M KCl) (as reference electrode). Tafel polarization and EIS were employed to measure the resistance of coating against corrosion in 3.5% NaCl solution. Prior to polarization tests, substrates were immersed in the above solution, and then the open circuit potential (OCP) was carefully observed to reach a fixed amount of potential. Potentiostat polarization and OCP were recorded through the use of PGSTAT204 equipment (MetrohmAutolab B.V., Netherlands). The potential of

potentiodynamic polarization was removed at a scan rate of 10 mVs^{-1}, in a potential limit of ±250 mV vs. OCP. To recognize the Tafel corrosion potential, two curves of anodic and cathodic polarization were obtained and then the regions were extrapolated to the corrosion potential (E_{corr}) to obtain corrosion current density (I_{corr}).

EIS was carried out using a frequency response detector (EG&G model 1025) with an electrochemical setup controlled by M 398 software. The range of frequencies to obtain EIS results were between 0.01 and 100,000 Hz. It should be noted that EIS tests were conducted at OCP. To evaluate the impedance spectra, the resulting experimental data was fitted into equivalent circuits with Zview software.

2.5. Microstructural and Electro-chemical Characterization

The crystalline structure of PMMA/PANI/Fe3O4 nanocomposite coating was studied by means of XRD analysis. The diffraction patterns of the PMMA/PANI/Fe3O4 was obtained with PHILIPS Diffractometer (D5000). The data were collected within 2Θ angle from 10° to 80° using Cu Kα line (λ = 0.15418 nm). The functional groups and structure of the PMMA/PANI/Fe3O4 nano-composite coating was determined by FT-IR. Infrared spectra in the range 400–4000 cm^{-1} on the sample pellets made with KBr were measured by using Bruker Tensor 27 spectrometer. SEM (Ziess MV2300) and TEM (Ziess 80 kV) analyses were adopted to characterize the morphologies of PMMA/PANI/Fe3O4 nanocomposite coating through the use of an LEO 1455 UP analyzer (Ziess MV2300). An AUTOLAB model PGSTAT30 was employed to run corrosion inhibition electrochemical tests of the PMMA/PANI/Fe3O4 nano-composite coating containing EIS and Tafel polarization. EIS studies were performed at corrosion potentials (E_{corr}) over a frequency range of 10 kHz-0.1 Hz with a signal amplitude perturbation of 0.5 mV. Then impedance data were analyzed through a Pentium IV computer and FRA software. A scan rate of 0.5 mV s^{-1} was set during the Tafel polarization. The obtaining data were investigated by the GPES electrochemical software [23].

3. RESULT AND DISCUSSIONS

3.1. Characterization of Synthesized Nanocomposites

XRD spectra of the synthesized nanocomposite coating are shown in Figure 2. Looking at this figure, the strong Bragg peaks of PMMA/PANI/Fe3O4 revealed at angles of 2Θ ≃ 22° to 31° in the spectrum. These peaks demonstrate that the crystalline structure of PMMA/PANI/Fe3O4 nano-composites was obtained, showing the regular arrangement of copolymer chains by chain-folding. Furthermore, this pattern indicates the structure of PANI/Fe_3O_4 nanocomposites were not changed during the preparation process [24, 25].

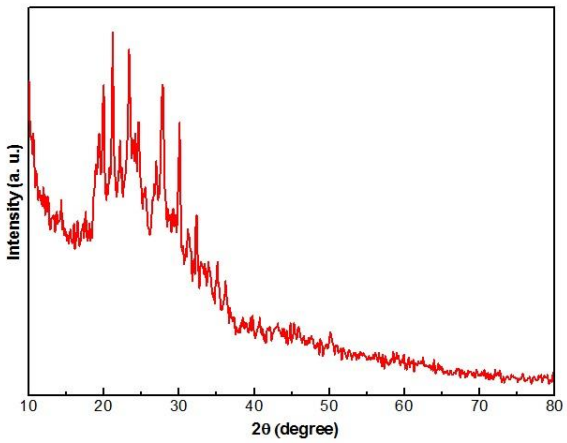

Figure 2. *XRD diffraction patterns of PMMA/PANI/Fe3O4 nanocomposite coating.*

FTIR pattern was used to characterize PMMA/PANI/Fe3O4 nanocomposite coating. Therefore, FTIR pattern of the synthesized nanocomposites was plotted in the range of 400-4000 cm^{-1}, presented in Figure 3. In this figure, the adsorption peak located at 592 cm^{-1} was the characteristic peak of Fe–O bond which proving the presence of Fe_3O_4 nanoparticles in the synthesized nanocomposites. Regarding PANI characteristic peaks, the peak

observed at around 3500 cm^{-1} was assigned to the N–H stretching. In addition, the adsorption bonds located at approximately 1500 cm^{-1} were ascribed to quinine ring and benzene ring of PANI. The presence of –CH_3-substituted and C–N stretching adsorption groups in PANI structure were detected via the peaks occurred at 1296 cm^{-1} and 1301 cm^{-1}. The sharp peak observed at 1633 cm^{-1} was assigned to C=O groups of PMMA. Furthermore, the bands in the 2800-3000cm^{-1} region were from the stretching of C–H bonds of the saturated alkane existing in PMMA structure, confirming the presence of PMMA. According to these observations, PMMA resin and PANI/Fe_3O_4 nanocomposites were shown to be present in the synthesized nanocomposites [26-28].

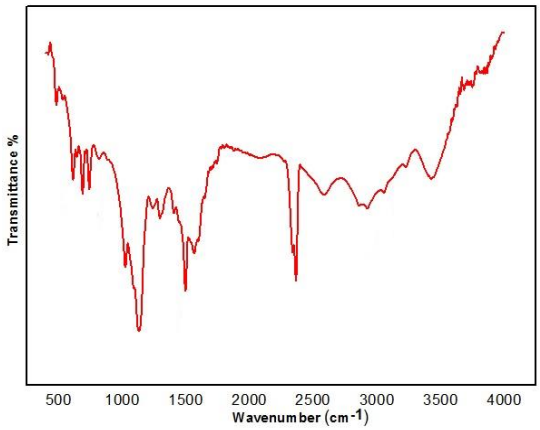

Figure 3. *The FTIR spectra of MMA/PANI/Fe3O4 nanocomposite coating.*

The thermal stability of PMMA/PANI/Fe_3O_4 nanocomposites was investigated via TGA analyses. To establish a balance, nitrogen was employed as the purge gas. Data were collected from the ambient temperature to 700°C at a rate of 10 °C min^{-1}. Moreover, the curve of the weight loss percentage versus temperature were plotted. In Figure 4, the TGA plot of PMMA/PANI/Fe_3O_4 in the atmospheric condition shows that 59.61wt% of PMMA/PANI/Fe_3O_4 nanocomposite coat-ing was entirely decomposed at high temperatures (higher than 500°C. The first signs of thermal transition were observed at 125-275°C, where the first weight loss at a lower temperature is primarily because of the elimination of moisture (up to 125°C) and dopant anions (275°C). In addition, the main thermal decomposition for PMMA/PANI/Fe3O4 nanocomposite composites coating occurred around 300 and 500°C. The degradation of this nanocomposite coating might occur due to the weak head-to-head bonding, solvent and impurities in the nanocomposites [29, 30].

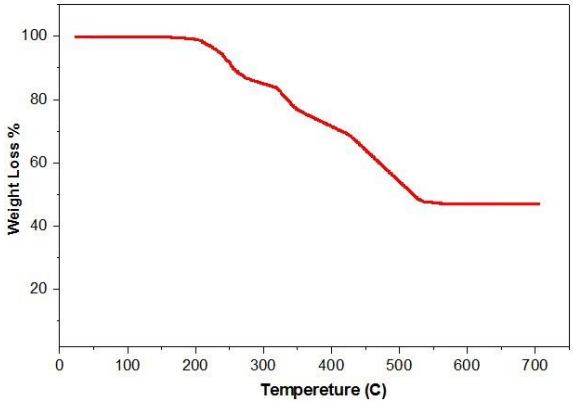

Figure 4. *TGA curve of PMMA/PANI/Fe3O4 nanocomposite coating.*

The surface morphology of PMMA/PANI/Fe_3O_4 nanocomposite coating was identified by means of TEM and SEM analyses. Figure 5, SEM image, depicts that PMMA/PANI/Fe_3O_4 nanocomposite coating had a smooth surface with somehow spherical structure. Moreover, this image illustrates that the PANI and Fe_3O_4 were evenly dispersed in the PMMA acrylic resin. That is to say, Fe_3O_4 nanoparticles were strongly adhered to the polymeric networks formed by PANI and PMMA.

TEM image of PMMA/PANI/Fe3O4 nanocomposite coating is shown in Figure 6. Overall, as stated above, TEM image confirms the formation of a core-shell structure. As can be seen in the Figure 6, a pale-colored layers of PANI and PMMA were coated on the dark core of Fe_3O_4 magnetic nanoparticle, with a thin coating layer of about 20 nm.

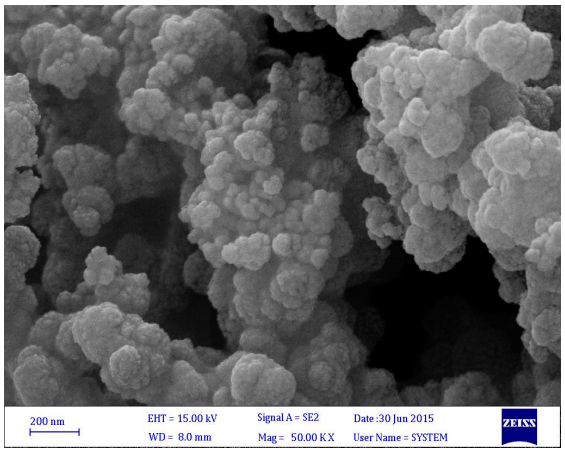

Figure 5. *SEM image of PMMA/PANI/Fe3O4 nanocomposite coating.*

Moreover, this image confirms that PMMA completely covered PANI/Fe_3O_4 and the average size of the PMMA/PANI/Fe3O4 nanocomposite coating microspheres was about 30 nm.

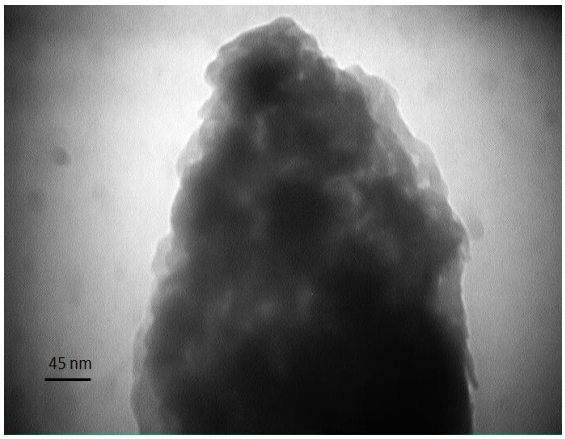

Figure 6. *TEM analysis of PMMA/PANI/Fe3O4 nanocomposite coating.*

3.2. Potentiodynamic Polarization Studies

The corrosion resistance of the coating was evaluated through cyclic potentio-dynamic polarization measurements. Figure 7 presents the typical potentiodynamic polarization curves achieved from the industrial alkyd paint without coating and modified alkyd paint with different contents of PMMA/PANI/Fe3O4 coated mild steel substrates in a 3.5% NaCl solution. The values of b_a and b_c (Tafel slopes), Ecorr (corrosion potential), I_{corr} (corrosion current), R_p (polarization resistance) obtained from extrapolation of Tafel plot and η_p (protection efficiency) are listed in Table 1. The equation below was used to obtain the protection efficiency of coating:

$$\eta_p = \frac{I_{corr} - I_{corr(c)}}{I_{corr}} \qquad (1)$$

where I_{corr} and $I_{corr(c)}$ are the corrosion currents in the absence and the presence of a coating, respectively.

Obtained results revealed that the corrosion potential of coated samples shifted towards more positive values. This positive change of E_{corr} was an indication of anodic protection of the mild steel surface by the implemented coatings. According to the Tafel plots in Figure 7, a significant reduction in both cathodic and anodic currents was observed when mild steel was coated with the modified alkyd paint. These types of coating curbed the anodic and cathodic reactions of mild steel in an aggressive medium, so that the I_{corr} values declined from 5.82×10^{-6} A/cm^2 for bare mild steel to 1.80×10^{-8} A/cm^2 for 6% PMMA/PANI/Fe3O4 sample, resulted in a desirable η_p of above 99%. These findings indicate that I_{corr} was considerably dependent on the nanocomposite percentage; that is to say 6% nanocomposite generated the lowest I_{corr}, while I_{corr} for samples containing 9 and 12% nanocomposites were much higher (8.03×10^{-8} and 1.64×10^{-7}, respectively). Such observations could be due to the different conductivity and porosity properties of coating used. It can be stated that in the case of 6% PMMA/PANI/Fe3O4 coating, nanocomposites were uniformly dispersed on the surface of the substrate mild steel, in comparison with the samples with higher compositions. This means that the proper dispersion, without agglomeration, led to a better conductivity in the resulting coating layer and that is why the corresponding I_{corr} and η_p were the most desirable among other samples.

Table 1. *Corrosion parameter obtained from Tafel plots for bare mild steel, industrial paint, and different composition PMMA/PANI/Fe3O4 nanocomposite modified paint.*

Sample	b_a (V/dec)	b_c (V/dec)	E_{corr} (V)	I_{corr} (A/cm^2)	R_P (Ω)	η_p
Bare Steel	0.26342	0.18093	-0.10624	5.82×10^{-6}	10190	-
IP	0.42403	0.34367	-0.045585	2.07×10^{-7}	508140	0.96443
IP+NP (3%)	0.52771	0.26261	-0.062624	1.89×10^{-8}	5.13×10^{6}	0.99675
IP+NP (6%)	0.48796	0.33243	-0.099016	1.80×10^{-8}	6.07×10^{6}	0.99691
IP+NP (9%)	0.40299	0.30309	-0.086641	8.03×10^{-8}	1.19×10^{6}	0.98620
IP+NP (12%)	0.52983	0.3142	-0.068774	1.64×10^{-7}	665890	0.97182

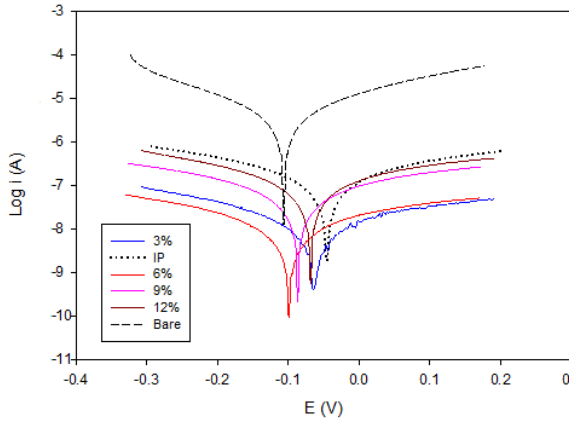

Figure 7. *Tafel plots for bare mild steel, industrial paint, and different composition PMMA/PANI/Fe3O4 nanocomposite modified paint.*

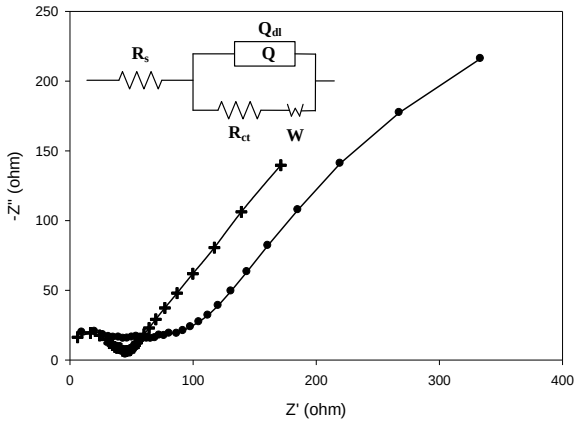

Figure 8. *Nyquist plots of (✚) industrial paint and (●) Pure PMMA/PANI/Fe3O4 nanocomposite coated mild steel in 3.5% NaCl solution.*

Figure 8 illustrate Nyquist plots of industrial paint and pure PMMA/PANI/ Fe3O4 nanocomposite coating. In addition, obtained Nyquist plots of PMMA/PANI/ Fe3O4 nanocomposite coating with various compositions in 3.5% NaCl solution are depicted in Figure 9. Impedance data for samples were fitted with equivalent circuit models and are indicated in the insets of Figure 8 and Figure 9. In the equivalent circuits models, R_s stands for the resistance of the solution, R_{ct} indicates the charge transfer resistance at high frequencies, R_f shows the film resistance of the adsorption of inhibitor molecules and all other accumulated species at metal-solution interface in the low-frequency region, Q_{dl} and Q_f are the constant phase elements (CPE), representing double-layer capacitance and film capacitance, respectively, and W is the Warburg impedance [31].

The values related to the representative parameters of the optimal fit to the obtained data by the two circuit models are summarized in Table 2. According to Table 2, the R_{ct} value increased from 38.3 Ωcm^2 for the industrial paint to 76.04, 329.8, 1027, 1685 and 280.6 Ωcm^2 for the pure nanocomposite and 3, 6, 9 and 12% nanocomposite coated samples, respectively. A consistent and flawlessly coated metallic surface can be identified by higher R_{ct} and R_f and lower Q_{dl} and Q_f [32]. The higher R_{ct} and R_f, and the lower Q_{dl} and Q_f for nanocomposite-modified paint indicated that the presence of the nanocomposites with 6-9% composition resulted an excellent corrosion performance for mild steel.

Table 2. *The EIS parameters of industrial paint and different composition PMMA/PANI/Fe3O4 nanocomposite modified paint.*

Sample	R_s (Ωcm^2)	Q (Fcm^{-2})	N	R_f (Ωcm^2)	Q (Fcm^{-2})	n	R_{ct} (Ωcm^2)	W (Ωcm^2)
IP	4.2	-	-	-	4.32×10^{-7}	0.878	38.3	1.98×10^{-2}
NP	9.7	-	-	-	3.74×10^{-5}	0.524	76.04	1.06×10^{-2}
IP+NP (3%)	20.04	3.20×10^{-8}	0.82	60.88	2.90×10^{-3}	0.48	329.8	6.24×10^{-4}
IP+NP (6%)	21.59	3.57×10^{-9}	0.9	57.11	4.04×10^{-4}	0.49	1027	4.57×10^{-4}
IP+NP (9%)	16.15	2.74×10^{-9}	0.88	50.02	3.1×10^{-4}	0.43	1685	2.89×10^{-4}
IP+NP (12%)	15.85	2.1×10^{-8}	0.86	35.4	1.46×10^{-4}	0.48	280.6	2.52×10^{-4}

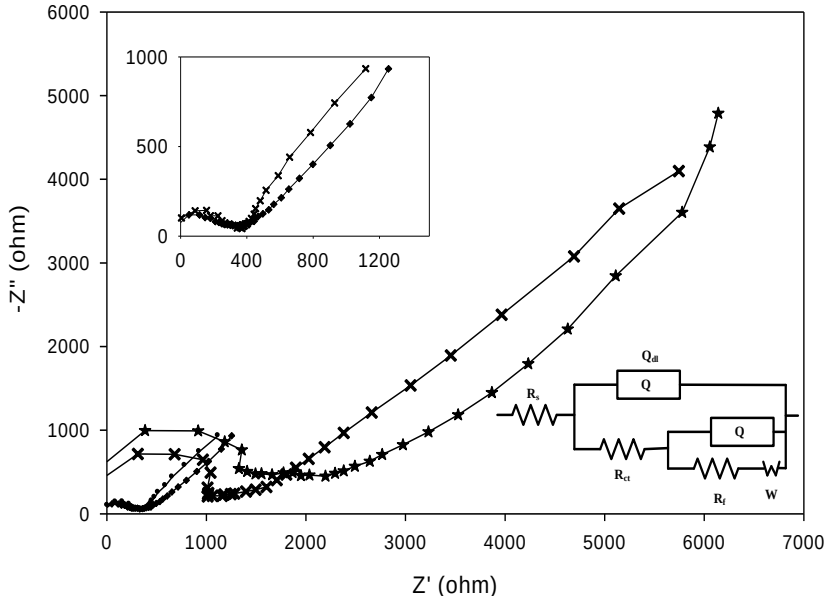

Figure 9. *Nyquist plots of different compositions of PMMA/PANI/Fe3O4 nanocomposite modified paint in 3.5% NaCl solution, (●) 3% nanocomposite, (×) 6% nanocomposite, (★) 9% nanocomposite, (◆) 12% nanocomposite.*

Table 3 represents a comparison of corrosion resistance of various polyaniline coatings. Compared with other works, according to the Icorr, Ecorr and the anticorrosion efficiency, prepared coating in this work has a good barrier effect on corrosion of mild steel.

3.3. Anticorrosion Mechanism

It is generally accepted that the steel corrosion process includes reduction and oxidation reaction which are summarize as below [33]:

$$Fe \rightarrow Fe^{2+} + 2e^- \quad (2)$$

$$Fe^{2+} \rightarrow Fe^{3+} + e^- \quad (3)$$

$$O_{2\,(g)} + 2H_2O + 4e^- \rightarrow 4OH^- \quad (4)$$

$$2Fe^{2+}_{(aq)} + O_{2\,(g)} + 2H_2O \rightarrow 2FeOOH + 2H^+ \quad (5)$$

As it is obvious, the corrosion process of mild steel is considerably related to the presence of enough O_2 and H_2O. To halt or

slow down one of these reactions would be effective when it comes to protecting the substrate mild steel from rust formation. For that reason, a desirable coating agent should effectively be capable of retarding these reactions, which generally done via physical or electrochemical protection [34].

Table 3. *A summary of studies about PANI nanocomposites in enhancing the corrosion resistance of coatings.*

Materials	Substrate	Icorr (μA cm–2)	Ecorr (mV)	Efficiency (%)	Reference
polyaniline–SiO2	mild steel	0.09	-	99.93	[35]
polyaniline/graphene	mild steel	0.38	−537	53.49	[36]
Polyaniline-clay- epoxy	mild steel	0.061	−664	76.20	[37]
PANI-Fe2O3- alkyd resin	mild steel	1.8	−962	-	[38]
Polyaniline-Boron nitride-PVA	mild steel	1.03	−44	90.95	[39]
This work	mild steel	0.018	−99	99.69	

As a superb coating material, PMMA /PANI/Fe3O4 nanocomposites protected the surface of mild steel via the formation of an impermeable layer upon its surface, referred to as physical protection. This means that the protecting layer served a crucial role in inhibiting the diffusion of corrosive agents, such as O_2 and electrolyte molecules, to the surface of mild steel through the formation of a physical barrier. Furthermore, in terms of electrochemical protection, the existing PANI/PMMA in the nanocomposite coating structure might take part in electrochemical corrosion reactions, retarding the corrosion of underlying steel. In other words, it was PANI/PMMA molecules that constantly reduced and oxidized in cyclic electrochemical reactions instead of the substrate mild steel layer, as a result of which the substrate was intact and protected against corrosion reactions.

4. CONCLUSION

In this paper, the anti-corrosion ability of modified industrial alkyd paint with PMMA/PANI/Fe3O4 nanocomposites on mild steel was studied. The corrosion behavior of coated mild steel was evaluated via potentiodynamic polarization and EIS techniques, both conducted in 3.5% NaCl solutions. Firstly, PMMA/PANI/Fe3O4 nanocomposites were synthesized. Through characterization procedures, namely XRD, FTIR, SEM, TEM and TGA, the nanocomposites were elementally, morpho-logically and thermally analyzed. Afterward, the modifying effects of the synthesized nanocomposites were studied by means of Tafel polarization and EIS methods, in which the nanocomposites were blended with industrial alkyd pain. Based on these methods, 6% PMMA/PANI/ Fe3O4 nanocomposite coating produced significant protection against corrosion; with I_{corr} of 1.80×10^{-8} A/cm^2 and η_p of more than 99%. As a result, PMMA/PANI/ Fe3O4 nanocomposites could be recommended as a promising coating material, and one will achieve desirable corrosion results when blending these with industrial alkyd paint, particularly, for mild steel protecting purposes.

CONFLICT OF INTEREST

The authors declare that they have no conflict of interest.

REFERENCES

1. Mohammadzadeh, A., Taleghani, H. G., Lashkenari, M. S., "Preparation and comparative study of anticorrosion nanocomposites of polyaniline/graphene oxide/clay coating", *J. Mater. Res. Technol.*, 13 (2021) 2325-2335.
2. Lin, Y., Singh, A., Ebenso, E. E., Wu, Y., Zhu, C., Zhu, H., "Effect of poly (methyl methacrylate-co-N-vinyl-2-pyrrolidone) polymer on J55 steel corrosion in 3.5% NaCl solution saturated with CO 2", *J. Taiwan Inst. Chem. Eng.*, 46 (2015) 214-222.
3. Layeghi, R., Farbodi, M., Ghalebsaz-Jeddi, N., "Preparation of polyaniline-polystyrene-ZnO nanocomposite and characterization of its anti-corrosive performance", *Int. J. Nanosci. Nanotechnol.*, 12 (2016) 167-174.
4. Bilal, S., Gul, H., Gul, S., "One Pot Synthesis of Highly Thermally Stable Poly (2-Methylaniline) for Corrosion Protection of Stainless Steel", *Iran. J. Sci. Technol. Trans A. Sci.*, 42 (2018) 1915-1922.
5. Shah, A.-u.-H. A., Kamran, M., Bilal, S., Ullah, R., "Cost effective chemical oxidative synthesis of soluble and electroactive polyaniline salt and its application as anticorrosive agent for steel", *Materials*, 12 (2019) 1527.
6. Yeganeh, M., Marashi, S., Mohammadi, N., "Smart corrosion inhibition of mild steel using mesoporous silica nanocontainers loaded with molybdate", *Int. J. Nanosci. Nanotechnol.*, 14 (2018) 143-151.
7. Qiu, S., Chen, C., Zheng, W., Li, W., Zhao, H., Wang, L., "Long-term corrosion protection of mild steel by epoxy coating containing self-doped polyaniline nanofiber", *Synth. Met.*, 229 (2017) 39-46.
8. Jafari, Y., Ghoreishi, S., Shabani-Nooshabadi, M., "Polyaniline/graphene nanocomposite coatings on copper: electropolymerization, characterization, and evaluation of corrosion protection performance", *Synth. Met.*, 217 (2016) 220-230.
9. Hosseini, M., Shahryari, E., Najjar, R., Ahadzadeh, I., "Study of super capacitive behavior of polyaniline/manganese oxide-carbon black nanocomposites based electrodes", *Int. J. Nanosci. Nanotechnol.*, 11 (2015) 147-157.
10. Ray, S., Easteal, A. J., Cooney, R. P., Edmonds, N. R., "Structure and properties of melt-processed PVDF/PMMA/polyaniline blends", *Mater. Chem. Phys.*, 113 (2009) 829-838.
11. Rahman, S. U., Bilal, S., "Synthesis and Characterization of Polyaniline-Chitosan Patches with Enhanced Stability in Physiological Conditions", *Polymers*, 12 (2020) 2870.
12. Lu, H., Hu, Y., Gu, M., Tang, S., Lu, H., Meng, X., "Synthesis and characterization of silica–acrylic–epoxy hybrid coatings on 430 stainless steel", *Surf. Coat. Technol.*, 204 (2009) 91-98.
13. Shi, S., Zhang, Z., Yu, L., "Hydrophobic polyaniline/modified SiO 2 coatings for anticorrosion protection", *Synth. Met.*, 233 (2017) 94-100.
14. Javidparvar, A., Ramezanzadeh, B., Ghasemi, E., "The effect of surface morphology and treatment of Fe3O4 nanoparticles on the corrosion resistance of epoxy coating", *J. Taiwan Inst. Chem. Eng.*, 61 (2016) 356-366.
15. Mammeri, F., Rozes, L., Sanchez, C., Bourhis, E. L., "Mechanical properties of SiO 2-PMMA based hybrid organic-inorganic thin films", *J. Sol-Gel Sci. Technol.*, 26 (2003) 413-417.
16. Alirezaei, S., Monirvaghefi, S., Salehi, M., Saatchi, A., "Wear behavior of Ni–P and Ni–P–Al 2 O 3 electroless coatings", *Wear*, 262 (2007) 978-985.
17. Afroukhteh, S., Dehghanian, C., Emamy, M., "Corrosion behavior of Ni–P/nano-TiC composite coating prepared in electroless baths containing different types of surfactant", *Progress in Natural Science: Materials International*, 22 (2012) 480-487.
18. Ramezanzadeh, B., Moghadam, M. M., Shohani, N., Mahdavian, M., "Effects of highly crystalline and conductive polyaniline/graphene oxide composites on the corrosion protection performance of a zinc-rich epoxy coating", *Chem. Eng. J.*, 320 (2017) 363-375.
19. Rahmanzadeh, L., Ghorbani, M., Jahanshahi, M., "Synthesis and Characterization of Fe3O4@ Polyrhodanine Nanocomposite with Core–Shell Morphology", *Adv. Polym. Tech.*, 33 (2014).
20. Muhammad, A., Bilal, S., "Comparative study of the adsorption of Acid Blue 40 on polyaniline, magnetic oxide and their composites: Synthesis, characterization and application", *Materials*, 12 (2019) 2854.
21. Aleahmad, M., Taleghani, H. G., Eisazadeh, H., "Preparation and characterization of PAn/NiO nanocomposite using various surfactants", *Synth. Met.*, 161 (2011) 990-995.
22. Bilal, S., Gul, S., Holze, R., "An impressive emulsion polymerization route for the synthesis of highly soluble and conducting polyaniline salts", *Synth. Met.*, 206 (2015) 131-144.
23. Ur Rahman, S., Röse, P., Krewer, U., Bilal, S., Farooq, S., "Exploring the Functional Properties of Sodium Phytate Doped Polyaniline Nanofibers Modified FTO Electrodes for High-Performance Binder Free Symmetric Supercapacitors", *Polymers*, 13 (2021) 2329.
24. Sharma, B. K., Gupta, A. K., Khare, N., Dhawan, S., Gupta, H., "Synthesis and characterization of polyaniline–ZnO composite and its dielectric behavior", *Synth. Met.*, 159 (2009) 391-395.
25. Muhammad, A., Shah, A.-u.-H. A., Bilal, S., Rahman, G., "Basic Blue dye adsorption from water using Polyaniline/Magnetite (Fe3O4) composites: Kinetic and thermodynamic aspects", *Materials*, 12 (2019) 1764.

26. Cao, Z., Jiang, W., Ye, X., Gong, X., "Preparation of superparamagnetic Fe 3 O 4/PMMA nano composites and their magnetorheological characteristics", *J. Magn. Magn. Mater.*, 320 (2008) 1499-1502.
27. Hong, R., Feng, B., Cai, X., Liu, G., Li, H., Ding, J., Zheng, Y., Wei, D., "Double-miniemulsion preparation of Fe3O4/poly (methyl methacrylate) magnetic latex", *J. Appl. Polym. Sci.*, 112 (2009) 89-98.
28. Röse, P., Krewer, U., Bilal, S., "An Amazingly Simple, Fast and Green Synthesis Route to Polyaniline Nanofibers for Efficient Energy Storage", *Polymers*, 12 (2020) 2212.
29. Ferriol, M., Gentilhomme, A., Cochez, M., Oget, N., Mieloszynski, J., "Thermal degradation of poly (methyl methacrylate)(PMMA): modelling of DTG and TG curves", *Polym. Degradation Stab.*, 79 (2003) 271-281.
30. Bilal, S., Farooq, S., Holze, R., "Improved solubility, conductivity, thermal stability and corrosion protection properties of poly (o-toluidine) synthesized via chemical polymerization", *Synth. Met.*, 197 (2014) 144-153.
31. Shen, S., Guo, X.-y., Li, C.-c., Wen, Y., Yang, H.-F., "The synergistic mechanism of phytic acid monolayers and iodide ions for inhibition of copper corrosion in acidic media", *RSC Advances*, 4 (2014) 10597-10606.
32. Shabani-Nooshabadi, M., Ghoreishi, S., Behpour, M., "Direct electrosynthesis of polyaniline–montmorrilonite nanocomposite coatings on aluminum alloy 3004 and their corrosion protection performance", *Corros. Sci.*, 53 (2011) 3035-3042.
33. Radhakrishnan, S., Siju, C., Mahanta, D., Patil, S., Madras, G., "Conducting polyaniline–nano-TiO2 composites for smart corrosion resistant coatings", *Electrochim. Acta*, 54 (2009) 1249-1254.
34. Hu, C., Li, Y., Kong, Y., Ding, Y., "Preparation of poly (o-toluidine)/nano ZnO/epoxy composite coating and evaluation of its corrosion resistance properties", *Synth. Met.*, 214 (2016) 62-70.
35. Kumar S, A., Bhandari, H., Sharma, C., Khatoon, F., Dhawan, S. K., "A new smart coating of polyaniline–SiO2 composite for protection of mild steel against corrosion in strong acidic medium", *Polym. Int.*, 62 (2013) 1192-1201.
36. Chang, C.-H., Huang, T.-C., Peng, C.-W., Yeh, T.-C., Lu, H.-I., Hung, W.-I., Weng, C.-J., Yang, T.-I., Yeh, J.-M., "Novel anticorrosion coatings prepared from polyaniline/graphene composites", *Carbon*, 50 (2012) 5044-5051.
37. Motlatle, A. M., Ray, S. S., Scriba, M., "Polyaniline-clay composite-containing epoxy coating with enhanced corrosion protection and mechanical properties", *Synth. Met.*, 245 (2018) 102-110.
38. Sumi, V., Arunima, S., Deepa, M., Sha, M. A., Riyas, A., Meera, M., Saji, V. S., Shibli, S., "PANI-Fe2O3 composite for enhancement of active life of alkyd resin coating for corrosion protection of steel", *Mater. Chem. Phys.*, 247 (2020) 122881.
39. Sarkar, N., Sahoo, G., Das, R., Prusty, G., Sahu, D., Swain, S. K., "Anticorrosion performance of three-dimensional hierarchical PANI@ BN nanohybrids", *Industrial & Engineering Chemistry Research*, 55 (2016) 2921-2931.